



Stiffened composite hypar shell roofs under free vibration: Behaviour and optimization aids

Sarmila Sahoo, Dipankar Chakravorty*

Department of Civil Engineering, Jadavpur University, Kolkata 700032, India

Received 28 July 2005; received in revised form 25 November 2005; accepted 14 January 2006

Available online 17 April 2006

Abstract

A perusal of the literature brings out the fact that research reports on the vibration characteristics of stiffened composite hypar shells are missing. The present paper combines an eight noded shell element with a three noded beam element to develop a finite element tool for solution of such problems. Benchmark problems are solved to validate the approach and free vibration response of stiffened composite hypar shells is studied both with respect to fundamental frequency and mode shapes by varying the number and depth of stiffeners, laminations and boundary conditions. The results are further analysed to suggest guidelines to select optimum stiffened shell configurations considering the different practical constraints.

© 2006 Elsevier Ltd. All rights reserved.

1. Introduction

Among the common civil engineering shell forms which are used as roofing units, the skewed hypars have a special position because these architecturally pleasant forms may be cast and fabricated conveniently being doubly ruled surfaces. The hypar shells may be stiffened to have enhanced rigidity when subjected to point loads or provided with cutouts for some service requirements. A comprehensive idea about their static and free vibration characteristics is essential for a designer for successfully applying these forms. Now-a-days researchers are emphasizing more on laminated composite shells realizing the strength and stiffness potentials of this advanced material.

Free vibration of orthogonally stiffened cylindrical shell panels was reported by Bardell and Mead [1] for isotropic material using wave propagation techniques in conjunction with the hierarchical finite element method. Later Mecitoğlu and Dökmeçi [2] used the collocation method to study the free vibration of isotropic stiffened shallow cylindrical panels. Response of such panels under blast loading was carried out by Olson [3] using both finite element and finite strip methods. Sinha and Mukhopadhyay [4] reported frequencies and mode shapes of stiffened isotropic cylindrical panels using finite element again. Super finite elements were used to obtain free vibration results of stiffened cylindrical panels by Jiang and Olson [5]. Vibration of shell roof panels were reported by Chakravorty and Bandyopadhyay [6] considering isotropic cylindrical shells and later

*Corresponding author.

E-mail address: dc_ju@yahoo.com (D. Chakravorty).

Nomenclature			
a, b	length and width of shell in plan	u_{sx}, w_{sx}	axial and transverse translational degrees of freedom at each node of X -stiffener element
b_{st}	width of stiffener in general	v_{sy}, w_{sy}	axial and transverse translational degrees of freedom at each node of Y -stiffener element
b_{sx}, b_{sy}	width of X and Y stiffeners, respectively	W_b	weight of bare shell
B_{sx}, B_{sy}	strain displacement matrix of stiffener element	W_{st}	weight of stiffened shell
c	rise of hypar shell	x, y, z	local coordinate axes
d_{st}	depth of stiffener in general	X, Y, Z	global coordinate axes
d_{sx}, d_{sy}	depth of X and Y stiffeners, respectively	z_k	distance of bottom of the k th ply from mid-surface of a laminate
e	eccentricity of stiffeners with respect to mid-surface of shell	α_{sx}, β_{sx}	rotational degrees of freedom at each node of X -stiffener element
e_{sx}, e_{sy}	eccentricities of X and Y stiffeners with respect to mid-surface of shell	α_{sy}, β_{sy}	rotational degrees of freedom at each node of Y -stiffener element
E_{11}, E_{22}	elastic moduli	$\delta_{sxi}, \delta_{syi}$	nodal displacement of stiffener element
G_{12}, G_{13}, G_{23}	shear moduli of a lamina with respect to 1, 2 and 3 axes of fibre	ϕ	angle of twist
h	shell thickness	ν_{12}, ν_{21}	Poisson's ratios
M_{sxx}, M_{syy}	moment resultants of stiffeners	ρ	density of material
n_p	number of plies in a laminate	ω	natural frequency
n_x, n_y	number of stiffeners along X and Y directions, respectively	$\bar{\omega}$	nondimensional natural frequency [= $\omega a^2(\rho/E_{11}h^2)^{1/2}$]
N_{sxx}, N_{syy}	axial force resultants of stiffeners	$\bar{\omega}_b$	nondimensional natural frequency of bare shell
Q_{sxxz}, Q_{syyz}	transverse shear resultants of stiffeners	$\bar{\omega}_{st}$	nondimensional natural frequency of stiffened shell
R_{xy}	radii of cross-curvature of hypar shell		
T_{sxx}, T_{syy}	torsion resultants of stiffeners		

by Chakravorty et al. [7,8] considering composite cylindrical, conoidal, elliptic and hyperbolic paraboloidal shells, but similar studies about skewed hypar roofs are missing. In a review paper by Sinha and Mukhopadhyay [9], it was clearly pointed out that until 1995, only the cylindrical configuration for stiffened shell panels received considerable attention. As the researchers became more inclined towards composite materials, a number of interesting papers came up dealing with free vibrations of stiffened composite shell panels, most of which used the finite element as the analytical tool. Among these papers, Goswami and Mukhopadhyay [10], Mukhopadhyay and Goswami [11], Prusty and Satsangi [12] worked on both cylindrical and spherical shells while Rikards et al. [13] took up cylindrical stiffened shell panels. Qatu [14,15] reviewed in detail the research papers on shell dynamics for both isotropic and composite materials and observed that among stiffened panels, only cylindrical and spherical forms received some attention, while information of other forms are scanty. Recently Nayak and Bandyopadhyay [16,17] carried out free vibration studies of isotropic stiffened shell panels in detail including stiffened hypar shells. Free and forced vibrations of unstiffened composite hypar shell was reported by Chakravorty et al. [18]. In two recent papers Sahoo and Chakravorty [19,20] presented results of static and free vibration analysis of composite hypar shells but without stiffeners. Vibration of stiffened composite hypar shells received limited attention only in a recent paper published by Nayak and Bandyopadhyay [21] considering biaxially stiffened, antisymmetrically laminated shells only. The cases of uniaxially stiffened shells and symmetric laminations were excluded.

An overall look at the volume of literature that has accumulated regarding stiffened shell panels reflects the fact that stiffened composite skewed hypar shells have not received due attention by researchers. This, no doubt, defines a wide area of research and the present paper aims to focus on the free vibration characteristics of stiffened graphite–epoxy composite hypar shells.

2. Mathematical formulation

2.1. Finite element formulation for shell

A laminated composite hypar shell of uniform thickness h (Fig. 1) and twist radius of curvature R_{xy} is considered. Keeping the total thickness the same, the thickness may consist of any number of thin laminae each of which may be arbitrarily oriented at an angle θ with reference to the X -axis of the coordinate system. An eight-noded curved quadratic isoparametric finite element (Fig. 2) is used. The five degrees of freedom taken into consideration at each node include two inplane and one transverse displacement and two rotations about the X and Y axes. Sahoo and Chakravorty [19] reported in an earlier paper the strain–displacement and constitutive relationships together with the systematic development of stiffness matrix for the shell element.

2.2. Finite element formulation for stiffener of the shell

Three noded curved isoparametric beam elements (Fig. 2) are used to model the stiffeners, which are taken to run only along the boundaries of the shell elements. In the stiffener element, each node has four degrees of freedom

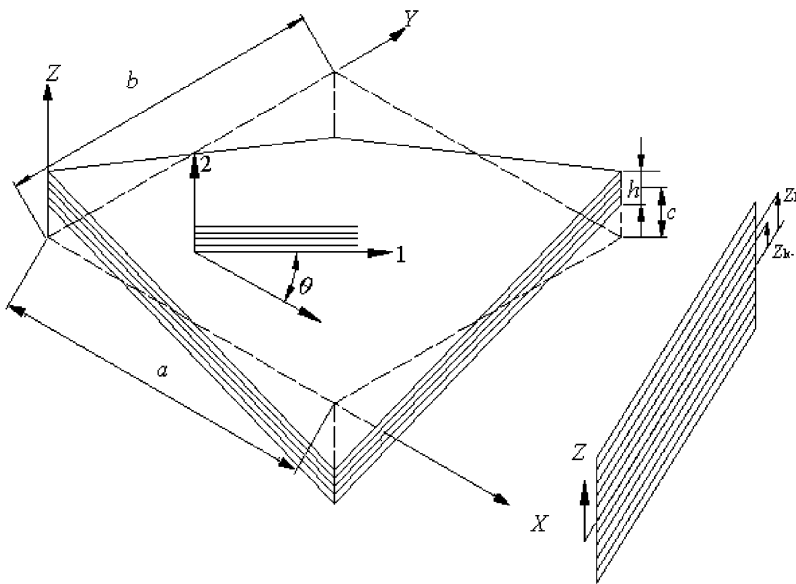


Fig. 1. Laminations in skewed hypar shell.

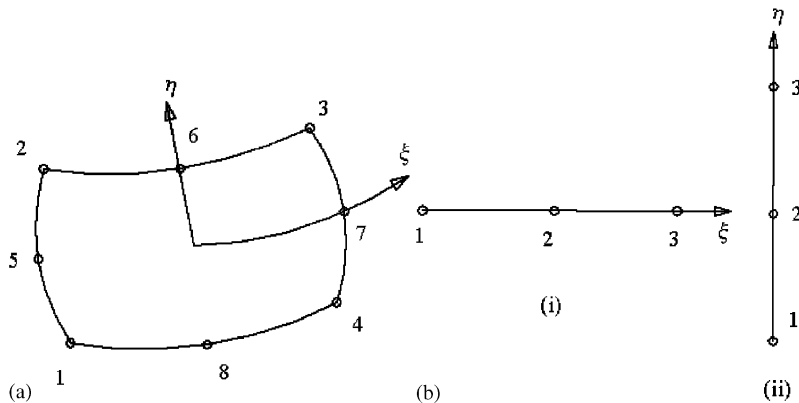


Fig. 2. (a) Eight noded shell element with isoparametric coordinates and (b) three noded stiffener element (i) X -stiffener (ii) Y -stiffener.

freedom i.e. u_{sx} , w_{sx} , α_{sx} and β_{sx} for X -stiffener and v_{sy} , w_{sy} , α_{sy} and β_{sy} for Y -stiffener. The generalized force-displacement relation of stiffeners can be expressed as (the notations have been defined in the nomenclature):

$$X\text{-stiffener} : \{F_{sx}\} = [D_{sx}]\{\epsilon_{sx}\} = [D_{sx}][B_{sx}]\{\delta_{sxi}\},$$

$$Y\text{-stiffener} : \{F_{sy}\} = [D_{sy}]\{\epsilon_{sy}\} = [D_{sy}][B_{sy}]\{\delta_{syi}\},$$

where

$$\{F_{sx}\} = \begin{bmatrix} N_{sxx} & M_{sxx} & T_{sxx} & Q_{sxxz} \end{bmatrix}^T, \quad \{\epsilon_{sx}\} = \begin{bmatrix} u_{sx,x} & \alpha_{sx,x} & \beta_{sx,x} & (\alpha_{sx} + w_{sx,x}) \end{bmatrix}^T$$

and

$$\{F_{sy}\} = \begin{bmatrix} N_{syy} & M_{syy} & T_{syy} & Q_{syyz} \end{bmatrix}^T, \quad \{\epsilon_{sy}\} = \begin{bmatrix} v_{sy,y} & \beta_{sy,y} & \alpha_{sy,y} & (\beta_{sy} + w_{sy,y}) \end{bmatrix}^T. \tag{1}$$

Elasticity matrices are as follows:

$$[D_{sx}] = \begin{bmatrix} A_{11}b_{sx} & B'_{11}b_{sx} & B'_{12}b_{sx} & 0 \\ B'_{11}b_{sx} & D'_{11}b_{sx} & D'_{12}b_{sx} & 0 \\ B'_{12}b_{sx} & D'_{12}b_{sx} & \frac{1}{6}(Q_{44} + Q_{66})d_{sx}b_{sx}^3 & 0 \\ 0 & 0 & 0 & b_{sx}S_{11} \end{bmatrix},$$

$$[D_{sy}] = \begin{bmatrix} A_{22}b_{sy} & B'_{22}b_{sy} & B'_{12}b_{sy} & 0 \\ B'_{22}b_{sy} & \frac{1}{6}(Q_{44} + Q_{66})b_{sy} & D'_{12}b_{sy} & 0 \\ B'_{12}b_{sy} & D'_{12}b_{sy} & D'_{11}d_{sy}b_{sy}^3 & 0 \\ 0 & 0 & 0 & b_{sy}S_{22} \end{bmatrix},$$

where

$$D'_{ij} = D_{ij} + 2eB_{ij} + e^2A_{ij}, \quad B'_{ij} = B_{ij} + eA_{ij}. \tag{2}$$

and A_{ij} , B_{ij} , D_{ij} and S_{ij} are explained in an earlier paper by Sahoo and Chakravorty [19].

Here the shear correction factor is taken as 5/6. The sectional parameters are calculated with respect to the mid-surface of the shell by which the effect of eccentricities of stiffeners is automatically included. The element stiffness matrices are of the following forms.

$$\text{for } X\text{-stiffener} : [K_{xe}] = \int [B_{sx}]^T [D_{sx}] [B_{sx}] dx,$$

$$\text{for } Y\text{-stiffener} : [K_{ye}] = \int [B_{sy}]^T [D_{sy}] [B_{sy}] dy. \tag{3}$$

The integrals are converted to isoparametric coordinates and are carried out by 2 point Gauss quadrature. Finally, the element stiffness matrix of the stiffened shell is obtained by appropriate matching of the nodes of the stiffener and shell elements through the connectivity matrix and is given as

$$[K_e] = [K_{she}] + [K_{xe}] + [K_{ye}]. \tag{4}$$

The element stiffness matrices are assembled to get the global matrices.

2.3. Element mass matrix

The element mass matrix for shell is obtained from the integral

$$[M_e] = \iint [N]^T [P] [N] dx dy, \tag{5}$$

where

$$[N] = \sum_{i=1}^8 \begin{bmatrix} N_i & 0 & 0 & 0 & 0 \\ 0 & N_i & 0 & 0 & 0 \\ 0 & 0 & N_i & 0 & 0 \\ 0 & 0 & 0 & N_i & 0 \\ 0 & 0 & 0 & 0 & N_i \end{bmatrix}, \quad [P] = \sum_{i=1}^8 \begin{bmatrix} P & 0 & 0 & 0 & 0 \\ 0 & P & 0 & 0 & 0 \\ 0 & 0 & P & 0 & 0 \\ 0 & 0 & 0 & I & 0 \\ 0 & 0 & 0 & 0 & I \end{bmatrix},$$

in which

$$P = \sum_{k=1}^{np} \int_{z_{k-1}}^{z_k} \rho \, dz, \quad \text{and} \quad I = \sum_{k=1}^{np} \int_{z_{k-1}}^{z_k} z \rho \, dz. \tag{6}$$

Element mass matrix for stiffener element

$$[M_{sx}] = \iint [N]^T [P] [N] \, dx \quad \text{for } X\text{-stiffener,}$$

and

$$[M_{sy}] = \iint [N]^T [P] [N] \, dy \quad \text{for } Y\text{-stiffener.} \tag{7}$$

Here $[N]$ is a 3×3 diagonal matrix.

$$[P] = \sum_{i=1}^3 \begin{bmatrix} \rho \cdot b_{sx} d_{sx} & 0 & 0 & 0 \\ 0 & \rho \cdot b_{sx} d_{sx} & 0 & 0 \\ 0 & 0 & \rho \cdot b_{sx} d_{sx}^2 / 12 & 0 \\ 0 & 0 & 0 & \rho (b_{sx} \cdot d_{sx}^3 + b_{sx}^3 \cdot d_{sx}) / 12 \end{bmatrix} \quad \text{for } X\text{-stiffener,}$$

$$[P] = \sum_{i=1}^3 \begin{bmatrix} \rho \cdot b_{sy} d_{sy} & 0 & 0 & 0 \\ 0 & \rho \cdot b_{sy} d_{sy} & 0 & 0 \\ 0 & 0 & \rho \cdot b_{sy} d_{sy}^2 / 12 & 0 \\ 0 & 0 & 0 & \rho (b_{sy} \cdot d_{sy}^3 + b_{sy}^3 \cdot d_{sy}) / 12 \end{bmatrix} \quad \text{for } Y\text{-stiffener.}$$

The mass matrix of the stiffened shell element is the sum of the matrices of the shell and the stiffeners matched at the appropriate nodes.

$$[M_e] = [M_{she}] + [M_{xe}] + [M_{ye}]. \tag{8}$$

The element mass matrices are assembled to get the global matrices.

2.4. Solution procedure for free vibration analysis

The free vibration analysis involves determination of natural frequencies from the condition

$$|[K] - \omega^2 [M]| = 0. \tag{9}$$

This is a generalized eigenvalue problem and is solved by the subspace iteration algorithm.

3. Numerical examples

A simply supported square plate with one stiffener in one plan direction is analysed applying the present formulation making the rise of the hyper shell zero. A comparison of the values of fundamental frequency obtained by Mukherjee and Mukhopadhyay [22], Nayak and Bandyopadhyay [17] and present method is presented in Table 1. Further a comparison of the nondimensional fundamental frequencies of cantilever

twisted plates obtained by Qatu and Leissa [23] and those obtained by the present method is furnished in Table 2.

Additional problems of stiffened skewed hypar shells (Fig. 3) are solved for eight different types of stacking sequences of shell surfaces, two different types of boundary conditions and four different types of stiffening schemes including bare shell with graphite-epoxy as the material. Among these combinations the symmetric angle-ply $[(+45^\circ / -45^\circ)_s]$ and antisymmetric angle-ply $[(+45^\circ / -45^\circ)_2]$ laminations perform best for simply supported and clamped boundaries, respectively. These shells are further analysed by varying the number of stiffeners in either or both of the plan directions up to ten. The symbols used to represent different laminations are: ASCP (antisymmetric cross-ply, $0^\circ/90^\circ, 0^\circ/90^\circ/0^\circ/90^\circ$), SYCP (symmetric cross-ply, $0^\circ/90^\circ/0^\circ, 0^\circ/90^\circ/90^\circ/$

Table 1
Natural frequencies (Hz) of centrally stiffened clamped square plate

Mode no.	Mukherjee and Mukhopadhyay [22]	Nayak and Bandyopadhyay [17]		Present method
		N8 (FEM)	N9 (FEM)	
1	711.8	725.2	725.1	733

$a = b = 0.2032$ m, shell thickness = 0.0013716 m, stiffener depth = 0.0127 m, stiffener width = 0.00635 m, stiffener eccentric at bottom. Material property: $E = 6.87 \times 10^{10}$ N/m², $\nu = 0.29$, $\rho = 2823$ kg/m³.

Table 2
Nondimensional natural frequencies ($\bar{\omega}$) for three-layer graphite-epoxy twisted plates, $[\theta / -\theta / \theta]$ laminate

Angle of twist (ϕ)	θ (deg)	0	15	30	45	60	75	90
15°	Qatu and Leissa [23]	1.0035	0.9296	0.7465	0.5286	0.3545	0.2723	0.2555
	Present FEM	0.9989	0.9258	0.7443	0.5278	0.3541	0.2720	0.2551
30°	Qatu and Leissa [23]	0.9566	0.8914	0.7205	0.5149	0.3443	0.2606	0.2436
	Present FEM	0.9491	0.8840	0.7181	0.5141	0.3447	0.2614	0.2445

$a/b = 1, a/h = 100; E_{11} = 138$ GPa, $E_{22} = 8.96$ GPa, $G_{12} = 7.1$ GPa, $\nu_{12} = 0.3$.

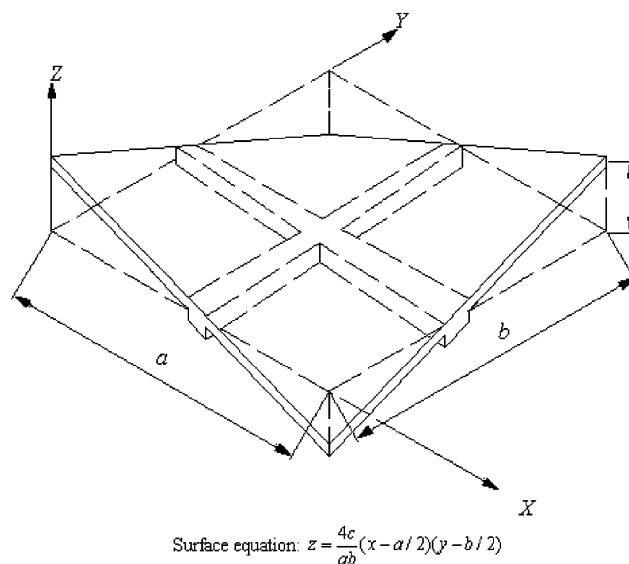


Fig. 3. A typical skewed hypar shell panel with biaxial stiffeners eccentric at shell bottom.

0°), ASAP (antisymmetric angle-ply, +45°/−45°, +45°/−45°/ +45°/−45°) and SYAP (symmetric angle-ply, +45°/−45°/ +45°, +45°/−45°/−45°/ +45°), etc. The individual lamina properties are assumed to be as $E_{11} = 25E_{22}$, $G_{12} = G_{13} = 0.5E_{22}$, $G_{23} = 0.2E_{22}$, $\nu_{12} = \nu_{21} = 0.25$. However, in all the cases the fibres in the stiffeners are considered to be arranged in a single layer along the length. In all the cases only the converged results are presented. The fundamental frequency is taken to have converged for particular finite element grid, if further refinement of the grid does not improve that result by more than 1%. With this criterion a 12×12 mesh is found to be appropriate for all the problems taken up here.

4. Results and discussions

The results of Table 1 show that the agreement of present results with the earlier ones is excellent and the correctness of the dynamic formulation is established. The fundamental frequencies of cantilever twisted plates obtained by Qatu and Leissa [23] compare well with the present results as furnished in Table 2 and the correctness of the present approach incorporating the effect of twist of curvature in the formulation is validated. Thus it is evident that the finite element model proposed here can successfully analyse vibration problems of stiffened skewed hypar composite shells which is reflected by close agreement of present results with benchmark ones.

4.1. Free vibration response of bare and stiffened hypars combining different laminations and boundary conditions

4.1.1. Fundamental frequency

Nondimensional fundamental frequencies for composite hypar shells with bare and stiffened surfaces are furnished in Tables 3 and 4 for simply supported (SSSS) and clamped (CCCC) boundary conditions, respectively. The laminations include two, three and four layered antisymmetric and symmetric, cross and angle plies. For this preliminary study only central stiffeners are considered running along either one or both of the plan directions. For all the laminations frequencies of *X*- and *Y*-stiffened shells are comparable for clamped boundary conditions. The same trend is almost true for simply supported boundary also. Only in the cases of 0°/90°/0° and 0°/90°/90°/0° laminates the *X*-stiffeners are found to impart considerably greater dynamic rigidity to a bare shell compared to the *Y*-stiffeners. In all the cases, however, a biaxially stiffened shell has greater frequency than one with a single stiffener. It is further noted that for cross-ply clamped shells the increase of frequency of a bare shell on stiffening is insignificant. An overall study of Tables 3 and 4 reveals that the angle-ply laminates yield higher frequencies than the cross-ply ones for both the boundary conditions. Four layered symmetric and antisymmetric angle-ply laminates appear to yield the highest frequencies among stacking orders considered presently for SSSS and CCCC stiffened surfaces, respectively.

Table 3
Nondimensional fundamental frequency of simply supported laminated composite hypar shells

Laminations	$n_x = 0, n_y = 0$	$n_x = 1, n_y = 0$	$n_x = 0, n_y = 1$	$n_x = 1, n_y = 1$
0°/90°	6.04644	6.10935	6.0659	7.60834
0°/90°/0°	6.47008	8.73346	6.47307	8.74104
0°/90°/0°/90°	7.72463	7.77772	7.72968	9.27972
0°/90°/90°/0°	6.92198	8.96514	6.92501	9.02681
+45°/−45°	5.97132	5.99681	5.97797	7.62406
+45°/−45°/+45°	8.53660	8.76874	8.80660	10.1723
+45°/−45°/+45°/−45°	8.54295	8.54607	8.55353	10.1763
+45°/−45°/−45°/+45°	8.9652	9.0858	9.1229	10.5489

$a/b = 1, a/h = 100, c/a = 0.2; E_{11} = 25E_{22}, G_{12} = G_{13} = 0.5E_{22}, G_{23} = 0.2E_{22}, \nu_{12} = \nu_{21} = 0.25, b_{st}/h = 1, d_{st}/h = 2$. Each stiffener has a single lamina with fibres along its length.

4.1.2. Mode shapes

The mode shapes of simply supported and clamped shells are presented in Figs. 4 and 5 considering the four layered laminates only. For unstiffened SSSS cross-ply shells the fundamental vibration modes are predominantly flexural with the nodal lines along the *Y* direction and hence *X*-stiffeners are found to be more effective than the *Y*-stiffeners in increasing the frequency. On the other hand for simply supported angle-ply unstiffened shells the *Y*-stiffeners are found to be more effective. The fundamental bending mode for the antisymmetric angle-ply shell has a nodal line along the *X* direction and hence the relatively higher frequency of the *Y*-stiffened shell is quite expected. Interestingly, the symmetric angle-ply simply supported shell with no stiffener or a pair of biaxial stiffeners show a bending mode along a diagonal direction which may be looked

Table 4
Nondimensional fundamental frequency of clamped laminated composite hypar shells

Laminations	$n_x = 0, n_y = 0$	$n_x = 1, n_y = 0$	$n_x = 0, n_y = 1$	$n_x = 1, n_y = 1$
0°/90°	17.2268	17.5550	17.5466	17.8214
0°/90°/0°	17.6786	17.9648	17.8316	18.2082
0°/90°/0°/90°	17.6069	17.9067	17.9067	18.1616
0°/90°/90°/0°	17.7269	18.0191	17.9912	18.2584
+45°/-45°	18.2576	19.5535	19.4445	25.5791
+45°/-45°/+45°	21.6202	23.4061	23.3884	28.4175
+45°/-45°/+45°/-45°	21.6021	24.1832	24.1341	29.7274
+45°/-45°/-45°/+45°	21.8578	23.9762	23.9714	28.7803

$a/b = 1, a/h = 100, c/a = 0.2; E_{11} = 25E_{22}, G_{12} = G_{13} = 0.5E_{22}, G_{23} = 0.2E_{22}, \nu_{12} = \nu_{21} = 0.25, b_{st}/h = 1, d_{st}/h = 2$. Each stiffener has a single lamina with fibres along its length.

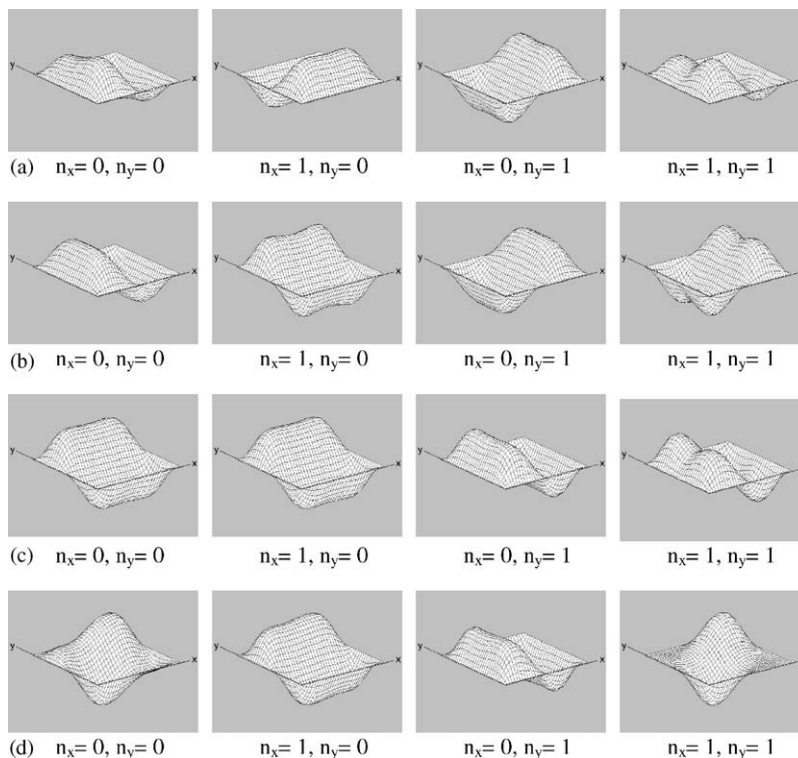


Fig. 4. Shapes for first mode of vibration of simply supported hypar shells with different arrangement of stiffeners and laminations (a) 0°/90°/0°/90° (b) 0°/90°/90°/0° (c) +45°/-45°/+45°/-45° (d) +45°/-45°/-45°/+45°.

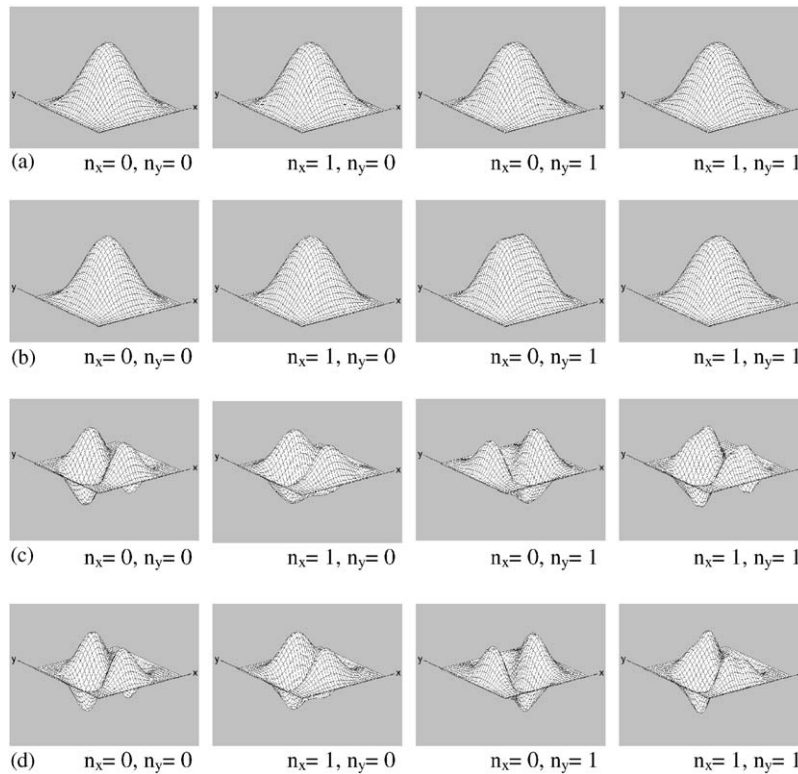


Fig. 5. Shapes for first mode of vibration of clamped hyper shells with different arrangement of stiffeners and laminations (a) $0^\circ/90^\circ/0^\circ/90^\circ$ (b) $0^\circ/90^\circ/90^\circ/0^\circ$ (c) $+45^\circ/-45^\circ/+45^\circ/-45^\circ$ (d) $+45^\circ/-45^\circ/-45^\circ/+45^\circ$.

upon as torsional modes of vibration along X and Y directions. In general, uniaxially stiffened shells have nodal lines along the stiffeners. Among the biaxially stiffened shells 3 out of 4 simply supported configurations (ASCP, SYCP and ASAP) have nodal lines along the Y direction.

For clamped shells both with and without stiffeners, nodal lines are less in number within the shell span compared to that for simply supported ones. The cross-ply clamped shells, both stiffened and unstiffened, show simple bending vibration modes along both the plan directions and provision of stiffeners either uniaxial or biaxial does not seem to have any major effect on the mode shapes and hence the performances of X - and Y -stiffeners are comparable. Interestingly, the angle-ply shells exhibit a greater amount of crests and troughs in the vibration modes. The symmetry of the shell geometry and laminations about the diagonals and the distribution of stiffeners parallel to the edges interact in a complex fashion giving rise to so many crests and troughs.

4.2. Effect of different stiffener arrangements on fundamental frequency

4.2.1. Fundamental frequency

The above study shows that among the simply supported shells the four layered symmetric angle-ply seems to be the best choice among all the laminations taken up here for both the bare and stiffened shells. It may be noted that such an inference is true only among the laminations considered here. Further study with other stacking sequences may lead to some other findings. Hence this stacking order is further taken up to investigate the effect of number of stiffeners, which may vary from 1 to 10 in either or both of the directions, on the fundamental frequency. The results furnished in Table 5 reveal that for any given value of n_x (0 to 8) when n_y increases, the nondimensional fundamental frequency ($\bar{\omega}$) always increases upto $n_y = 8$. However, when n_y is varied beyond 8 for given value of $n_x = 9$ or 10, $\bar{\omega}$ sometimes shows a marginal change and even

Table 5

Nondimensional fundamental frequency of simply supported laminated composite hypar shell of 45°/−45°/−45°/45° lamination and different combinations of stiffener arrangements

$n_y \rightarrow$ $n_x \downarrow$	0	1	2	3	4	5	6	7	8	9	10
0	8.9652	9.1229	9.2975	9.4907	9.8528	10.0592	10.3995	10.5156	10.6818	10.7385	10.7763
1	9.0858	10.5489	10.8372	11.0671	11.4807	11.7362	12.1770	12.3299	12.5731	12.6334	12.7149
2	9.2578	10.8180	11.7484	12.1370	12.6206	12.9199	13.4453	13.6231	13.9173	13.9797	14.0938
3	9.4473	11.0462	12.1229	12.9424	13.6048	13.9575	14.5471	14.7424	15.0629	15.1249	15.2616
4	9.8012	11.4542	12.6026	13.5921	14.5807	15.0790	15.6627	15.8354	16.1023	16.1425	16.2806
5	10.0032	11.7050	12.8977	13.9402	15.0594	15.8676	16.6038	16.7789	17.0268	17.0520	17.2000
6	10.3352	12.1341	13.4108	14.5177	15.6295	16.5738	17.4272	17.6605	17.7431	17.7353	17.8637
7	10.4483	12.2810	13.5819	14.7058	15.7945	16.7370	17.5985	18.2791	18.5168	18.4319	18.6746
8	10.6120	12.5154	13.8650	15.0141	16.0499	16.9726	17.6788	18.4508	18.5499	18.6031	18.7027
9	10.6678	12.5729	13.9244	15.0724	16.0867	16.9952	17.6687	18.3635	18.5923	19.0473	18.8795
10	10.7063	12.6541	14.0378	15.2083	16.2235	17.1412	17.7953	18.5104	18.6378	18.8553	18.8673

$a/b = 1, a/h = 100, c/a = 0.2; E_{11} = 25E_{22}, G_{12} = G_{13} = 0.5E_{22}, G_{23} = 0.2E_{22}, \nu_{12} = \nu_{21} = 0.25, b_{st}/h = 1, d_{st}/h = 2$. Each stiffener has a single lamina with fibres along its length.

may show a decreasing tendency. Addition of stiffeners to a bare shell surface increases both its stiffness and mass. When increase of stiffness is more significant than mass addition, the fundamental frequency tends to increase. But if the mass contribution prevails over the stiffness contribution of the stiffeners the shell may suffer from a resulting flexibility and $\bar{\omega}$ may decrease. This explains the above observation. For the same reason when n_y is fixed between 0 and 5 or at 8 and n_x is increased, $\bar{\omega}$ increases monotonically but when n_y is fixed at 6, 7, 9 or 10, the variation of $\bar{\omega}$ with n_x is not always monotonic.

As evident from Table 5, for simply supported shells for almost all given values of n_x , $\bar{\omega}$ tends to attain a saturation when n_y exceeds 5 and a shell with $n_y = 5$ (for any given value of n_x except 7) has $\bar{\omega}$ equal to 90% or more than that of a shell with $n_y = 10$. For $n_x = 7$ above value is marginally less than 90% (89.63%). Hence it may be concluded that for any given value if n_x , providing more than 5 Y-stiffeners is of no practical use. In fact, in some cases ($n_x = 0$ or 1) a shell with 4 Y-stiffeners can attain a frequency more than 90% of that with $n_y = 10$. Interestingly for any given value of n_y also, 5 X-stiffeners may be regarded practically to be as efficient than 10 X-stiffeners according to the criterion mentioned above.

If one looks along the diagonal of Table 5 it becomes evident that among shells with $n_x = n_y = n$ (say), a shell with $n = 6$ has $\bar{\omega}$ more than 90% of that with $n = 10$ ($0.9 \times 18.8673 = 16.9806$). Other stiffener combinations where $n_x \neq n_y$ may yield $\bar{\omega}$ more than 16.9806 provided the number of stiffeners along either of the directions is not less than 4.

From Table 4 it is evident that among clamped stiffened shells, the four layered antisymmetric angle-ply shows the best performance. This is why a study with this lamination is carried out further for clamped shells in the same way by varying n_x and n_y as done for simply supported shells. The results are presented in Table 6. Here again it is found that keeping either of n_x or n_y fixed when the number of stiffeners in the other direction is increased $\bar{\omega}$ initially shows an increasing tendency but attains a constancy or may even decrease when the number of such stiffeners exceed a certain value. From a similar study and using the same criterion as is done for simply supported shells above it is found that for clamped shells for a given number of stiffeners in one direction there is no practical point in increasing the number of stiffeners in other direction beyond 3. It is also seen from the Table 6 that a shell with $n_x = n_y = 5$ has frequency (34.8715) more than 90% of that with $n_x = n_y = 10$ ($0.9 \times 37.8762 = 34.0886$). It is further noted that for shells with $n_x \neq n_y$, $\bar{\omega} = 34.0886$ may be attainable in some cases provided the numbers of stiffeners in both the directions are not less than 3.

4.2.2. Mode shapes

From Figs. 6 and 7 it is found that when uniaxially stiffened SSSS shells are considered (with one or more stiffeners) nodal lines are found to run through the shell centre parallel to the stiffeners. But for

Table 6

Nondimensional fundamental frequency of clamped laminated composite hypar shell of $+45^\circ/-45^\circ/+45^\circ/-45^\circ$ lamination and different combinations of stiffener arrangements

$n_y \rightarrow$ $n_x \downarrow$	0	1	2	3	4	5	6	7	8	9	10
0	21.6021	24.1341	24.6929	24.8307	24.9228	24.9155	24.9628	24.9234	24.9486	24.9031	24.9418
1	24.1832	29.7274	29.6278	29.5266	29.6866	29.7578	30.1070	30.1191	30.2298	30.1669	30.2183
2	24.7494	29.6832	30.9348	31.2071	31.6679	31.8505	32.5323	32.6145	32.9754	32.9041	33.0199
3	24.8763	29.5893	31.2522	32.0353	32.8273	33.1560	34.0517	34.2163	34.8153	34.7624	34.9391
4	24.9559	29.7642	31.7610	32.8901	33.8740	34.2963	35.2026	35.3991	36.0571	36.0290	36.2432
5	24.9468	29.8480	31.9723	33.2648	34.3578	34.8715	35.7760	36.0291	36.6846	36.7201	36.9048
6	24.9994	30.2195	32.7134	34.2437	35.3430	35.8324	36.5602	36.7443	37.2344	37.2432	37.4173
7	24.9598	30.2357	32.8086	34.4396	35.5904	36.1439	36.8170	37.0340	37.4490	37.5047	37.6188
8	24.9857	30.3360	33.1684	35.0675	36.2828	36.8087	37.3113	37.4370	37.7107	37.7069	37.8144
9	24.9376	30.2705	33.0926	35.0152	36.2777	36.8892	37.3767	37.5559	37.7793	37.8280	37.8730
10	24.9768	30.3184	33.2016	35.1829	36.4669	37.0262	37.4942	37.6058	37.8184	37.8038	37.8762

$a/b = 1$, $a/h = 100$, $c/a = 0.2$; $E_{11} = 25E_{22}$, $G_{12} = G_{13} = 0.5E_{22}$, $G_{23} = 0.2E_{22}$, $\nu_{12} = \nu_{21} = 0.25$, $b_{st}/h = 1$, $d_{st}/h = 2$. Each stiffener has a single lamina with fibres along its length.

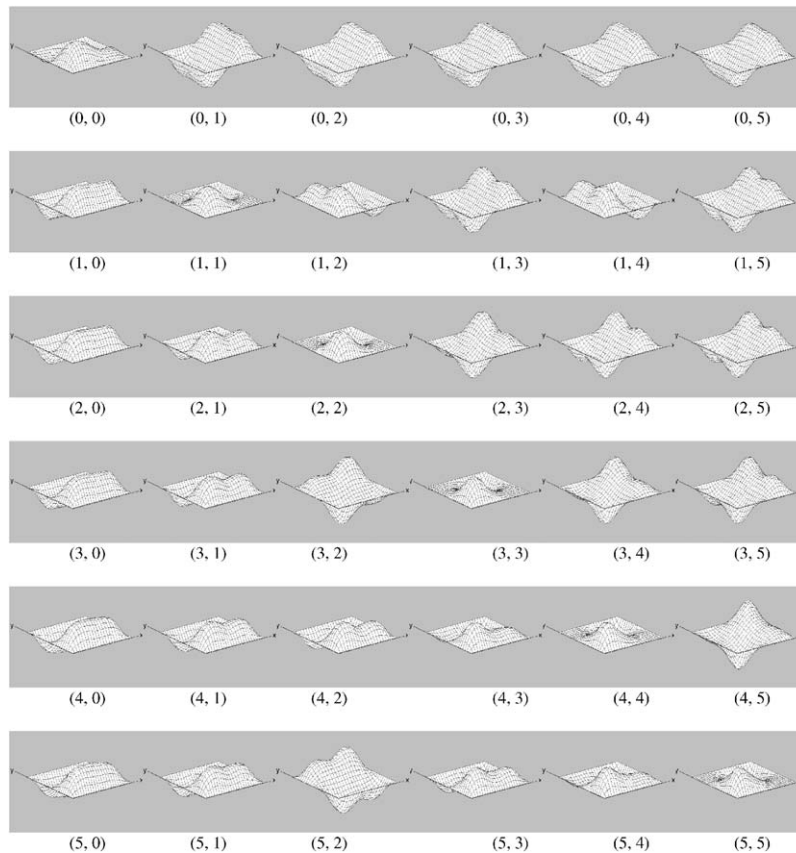


Fig. 6. Shapes for first mode of vibration of simply supported laminated ($+45^\circ/-45^\circ/-45^\circ/+45^\circ$) hypar shells with different numbers of stiffeners in each direction. Values in parentheses indicate (n_x, n_y) .

biaxially stiffened shells the vibration modes are complex. For clamped shells, however, nodal lines are not observed along the stiffeners among uniaxially stiffened shells. For simply supported shells some of the vibration modes are flexural along the diagonals and hence torsional along the X and Y directions.

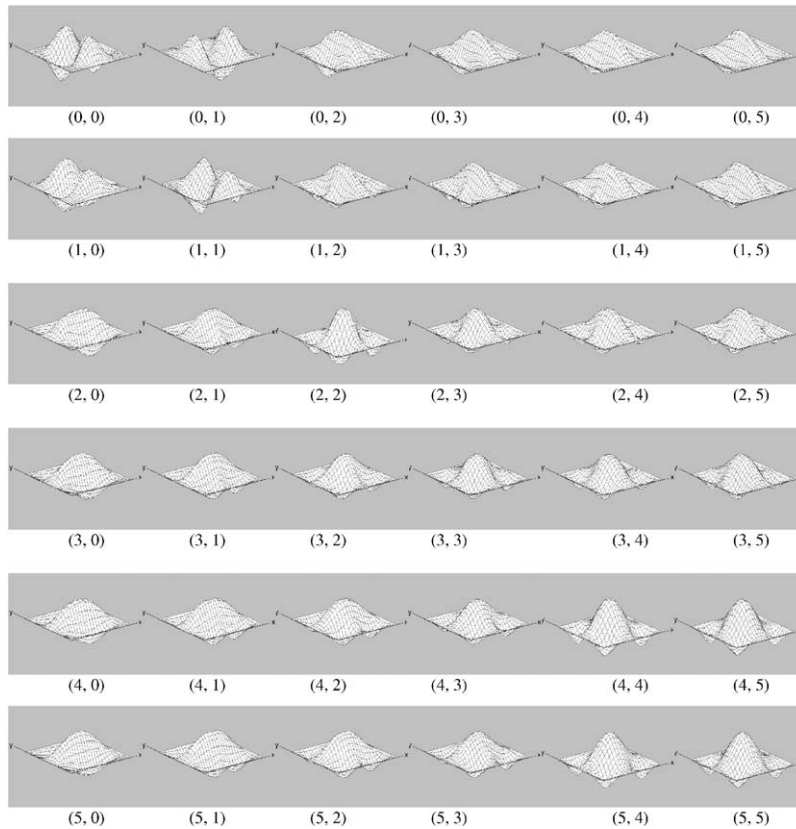


Fig. 7. Shapes for first mode of vibration of clamped laminated ($+45^\circ/-45^\circ/-45^\circ/+45^\circ$) hypar shells with different numbers of stiffeners in each direction. Values in parentheses indicate (n_x, n_y) .

For clamped shells such torsional modes of vibration are not observed and fundamental modes of vibration in all the cases are flexural along both the X and Y directions with a varying number of crests and troughs.

4.3. Effect of stiffener depth and number of biaxial stiffeners on fundamental frequency and guidelines for selection among different shell options

The variations of $\bar{\omega}$ with d_{st}/h ratio are presented in Fig. 8 for simply supported and clamped shells respectively with $n_x = n_y = n$ varying between 1 and 6. The graphs show that for any given value of n when the d_{st}/h ratio is increased the ratio of frequencies of stiffened and bare shells ($\bar{\omega}_{st}/\bar{\omega}_b = k$) initially increases but then attains a saturation for both the boundary conditions. For $n = 6$ such saturation values of k are 2.8 and 1.6 respectively for simply supported and clamped boundary conditions.

Table 7 is derived from Fig. 8 and furnishes the values of r (which is the ratio of weights of stiffened and bare shells) for different values of n and k . The values of d_{st}/h ratios are given in parentheses. If a particular value of k is unattainable for a given value of n the corresponding place of the table is left blank. It is found from the Table 7 that for any given value of k , there are different options of r and the minimum value of r among these is obviously the most economical solution provided the corresponding value of d_{st}/h ratio is not unacceptable due to consideration such as aesthetics and headroom. Interestingly, for any given value of k , although d_{st}/h decreases monotonically with n variation of r with n is quite arbitrary. In some cases a large value of d_{st}/h ratio combines with a small value of n to give economy (low value of r) and in some other situations a combination of a greater number of biaxial but shallow stiffeners seems to be most acceptable

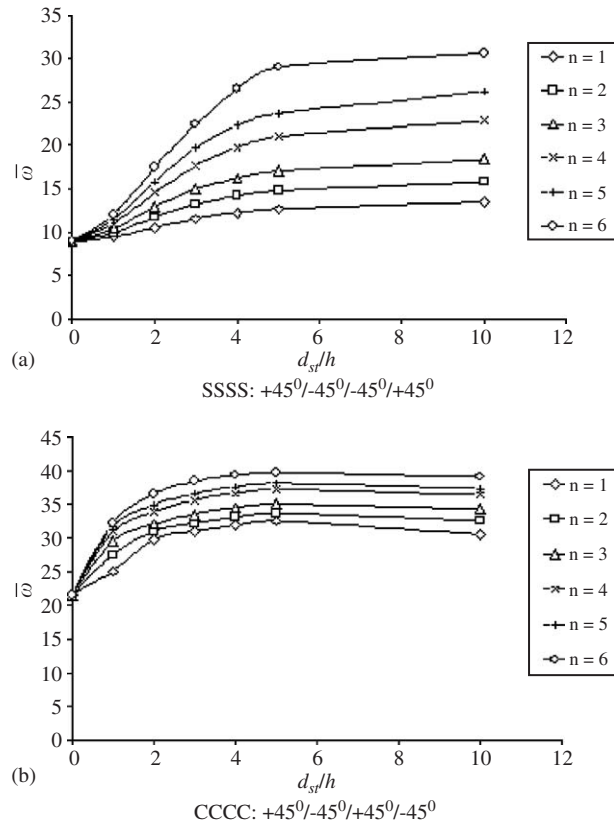


Fig. 8. Variation of nondimensional fundamental frequency with stiffener depth to shell thickness ratio for orthogonally stiffened composite hyarp shell.

Table 7

Weight ratios ($W_{st}/W_b = r$) of stiffened to bare shell for different values of frequency ratios ($k = \bar{\omega}_{st}/\bar{\omega}_b$) of stiffened to bare shell and $n_x = n_y = n$ (Ref. Fig. 8)

$k \rightarrow$ $n_x = n_y = n \downarrow$	Simply supported +45°/-45°/-45°/+45°						Clamped +45°/-45°/+45°/-45°					
	1.3	1.6	1.9	2.2	2.5	2.8	1.1	1.2	1.3	1.4	1.5	1.6
1	1.0645 (3.24)	—	—	—	—	—	1.1025 (0.63)	1.0231 (1.16)	1.0316 (1.59)	1.0460 (2.31)	1.0983 (4.94)	—
2	1.0768 (1.94)	1.1584 (4.0)	—	—	—	—	1.0123 (0.31)	1.0277 (0.70)	1.0420 (1.06)	1.0705 (1.78)	1.1338 (3.38)	—
3	1.0904 (1.53)	1.1531 (2.59)	1.2660 (4.5)	—	—	—	1.0112 (0.19)	1.0300 (0.50)	1.0443 (0.75)	1.0703 (1.19)	1.1294 (2.19)	1.2624 (4.44)
4	1.0972 (1.24)	1.1474 (1.88)	1.2078 (2.65)	1.3183 (4.06)	1.7542 (9.62)	—	1.0149 (0.19)	1.0321 (0.41)	1.0463 (0.59)	1.0737 (0.94)	1.1027 (1.31)	1.1835 (2.34)
5	1.1034 (1.06)	1.1580 (1.62)	1.2126 (2.18)	1.2925 (3.00)	1.4076 (4.18)	1.8375 (8.59)	1.0185 (0.19)	1.0400 (0.41)	1.0575 (0.59)	1.0819 (0.84)	1.1190 (1.22)	1.1862 (1.91)
6	1.1059 (0.91)	1.1641 (1.41)	1.2118 (1.82)	1.2875 (2.47)	1.3562 (3.06)	1.4214 (3.62)	1.0221 (0.19)	1.0361 (0.31)	1.0617 (0.59)	1.0908 (0.78)	1.1164 (1.00)	1.1676 (1.44)

The values in the parentheses are d_{st}/h ratios.

economically. Hence this table is expected to be very useful to practicing engineers to select a particular set of values of n and d_{st}/h to achieve a given value of k considering all the aspects of economy and other architectural and functional criteria.

Table 8

Values of $n_x = n_y = n$ for different values of frequency ratio of stiffened to bare shell ($k = \bar{\omega}_{st}/\bar{\omega}_b$) and d_{st}/h ratio

$k \rightarrow$ $d_{st}/h \downarrow$	Simply supported lamination: $+45^\circ/-45^\circ/-45^\circ/+45^\circ$						Clamped lamination: $+45^\circ/-45^\circ/+45^\circ/-45^\circ$					
	1.3	1.6	1.9	2.2	2.5	2.8	1.1	1.2	1.3	1.4	1.5	1.6
1.0	5 (1.0975)	—	—	—	—	—	1 (1.0199)	2 (1.0396)	3 (1.0591)	5 (1.0975)	—	—
1.5	3 (1.0887)	6 (1.1746)	—	—	—	—	1 (1.0299)	1 (1.0299)	2 (1.0594)	4 (1.1176)	6 (1.1746)	—
2.0	2 (1.0792)	4 (1.1568)	6 (1.2328)	—	—	—	1 (1.0398)	1 (1.0398)	1 (1.0398)	3 (1.1182)	4 (1.1568)	6 (1.2328)
2.5	2 (1.0990)	4 (1.1960)	5 (1.2438)	6 (1.2910)	—	—	1 (1.0498)	1 (1.0498)	1 (1.0498)	2 (1.0990)	4 (1.1960)	6 (1.2910)
3.0	1 (1.0597)	3 (1.1773)	4 (1.2352)	5 (1.2925)	6 (1.3492)	—	1 (1.0597)	1 (1.0597)	1 (1.0597)	2 (1.1188)	4 (1.2352)	5 (1.2925)
3.5	1 (1.0697)	3 (1.2955)	4 (1.2744)	5 (1.3413)	6 (1.4074)	—	1 (1.0697)	1 (1.0697)	1 (1.0697)	2 (1.1386)	4 (1.2744)	4 (1.2744)
4.0	1 (1.0796)	2 (1.1584)	4 (1.3136)	4 (1.3136)	5 (1.3900)	6 (1.4660)	1 (1.0796)	1 (1.0796)	1 (1.0796)	1 (1.0796)	3 (1.2364)	4 (1.3136)

Values in the parentheses indicate weight ratios (r) of stiffened shell to bare shell.

Table 8 presents the values of the number of biaxial stiffeners ($n_x = n_y = n$) in each direction for different values of the d_{st}/h ratio for which a particular value of k is just exceeded with the corresponding values of r in parentheses. This table is prepared taking practical upper limits of $d_{st}/h = 4.0$ and $n = 6$. For example for SSSS/SYAP boundary conditions when $d_{st}/h = 3.5$ and $n = 3$ the value of k just exceeds 1.6. A particular value of d_{st}/h ratio may not be sufficient to achieve a particular value of k since the upper limit of n is restricted to 6. The blank spaces in the table refer to such cases which means that for CCCC/ASAP shells the value of $k = 1.6$ is unattainable if $d_{st}/h = 1.0$ or 1.5. In order to attain a desired value of k an engineer may have practical limitations either in terms of headroom (d_{st}/h ratio) or in terms of number of stiffeners (n). In such situations Table 8 will be of great help to decide on the final selection of shell options keeping economy in consideration. If for SSSS/SYAP shells one has to attain $k \geq 1.6$ with $d_{st}/h \leq 3.5$, Table 8 shows that they have 14 options: (1) with $d_{st}/h = 1.5$ ($n = 6$), (2) with $d_{st}/h = 2.0$ ($n = 4, 6$), (3) with $d_{st}/h = 2.5$ ($n = 4, 5, 6$), (4) with $d_{st}/h = 3.5$ ($n = 3, 4, 5, 6$) and (4) with $d_{st}/h = 3.5$ ($n = 3, 4, 5, 6$). Of these combinations, the one with $d_{st}/h = 2.0$ and $n = 4$ is the most economical solution as it has the least value of r .

If in some other case for CCCC/ASAP shells an engineer has to attain $k \geq 1.4$ with $n \leq 4$ he has 13 choices: (1) with $d_{st}/h = 1.5$ ($n = 4$), (2) with $d_{st}/h = 2.0$ ($n = 3, 4$), (2) with $d_{st}/h = 2.5$ ($n = 2, 4$), (2) with $d_{st}/h = 3$ ($n = 2, 4$), (3) with $d_{st}/h = 3.5$ ($n = 2, 4, 4$) and (3) with $d_{st}/h = 4.0$ ($n = 1, 3, 4$). The designer can go for any of these options, and the one with $d_{st}/h = 4$ and $n = 1$ is the most economical choice.

In some critical situations an engineer may be encountered with restrictions both in terms of d_{st}/h ratio and n . If in the last case cited above the designer has both limitations of $n \leq 4$ and $d_{st}/h \leq 2.5$, Table 8 reveals that he has 5 options to attain $k \geq 1.4$ for CCCC/ASAP shells. These are with $d_{st}/h = 1.5$ ($n = 4$), $d_{st}/h = 2.0$ ($n = 3, 4$) and $d_{st}/h = 2.5$ ($n = 2, 4$). Among these choices, the option with $d_{st}/h = 2.5$ and $n = 2$ provides the maximum economy.

5. Conclusions

The following conclusions are drawn from the present study.

1. The finite element model used in the present paper may successfully solve the vibration problems of stiffened hypar shells and the results of the benchmark problems obtained by the present approach match well with the published ones.

2. If a designer has the limitation of providing only one central stiffener only he may preferably run the stiffeners along X direction because central X -stiffeners perform either equally or better than central Y -stiffeners for the class of laminations considered in the present study. For other laminations, however, this conclusion may not be true.
3. For effective increase of the fundamental frequency the stiffeners may be provided perpendicular to the nodal lines obtained from vibrations of bare shells. In the cases where no nodal lines are exhibited by a vibrating bare shell the performance of X - and Y -stiffeners are comparable.
4. The mode shapes of angle-ply shells are more complex than those of the cross-ply ones with greater number of crests and troughs within shell span among shells with a single central stiffener along one or both the plan directions.
5. For biaxially stiffened shells with one or more stiffener/s along each of the plan directions, the vibration modes for both the boundary conditions were found to be complicated. For some of the simply supported shells, torsional modes of vibration are identified while for clamped shells, the vibrational modes are flexural along both the plan directions.
6. With the increase of the number of stiffeners, either uniaxial or biaxial, the fundamental frequency increases but reaches a saturation whereafter there is no appreciable increase in frequency with the provision of additional stiffeners.
7. For any given number of stiffeners in one of the directions, there is no point in providing more than five or three stiffeners for simply supported and clamped shells respectively, along the other direction. Among shells with equal number of X - and Y -stiffeners there is no appreciable increase in frequency when the number of stiffeners in either direction exceeds 5.
8. The present study proves that there are two ways of increasing the fundamental frequency of a bare shell by stiffening, either by increasing the stiffener depth keeping the number of stiffeners fixed or by increasing the number of stiffeners with a given stiffener depth. Table 7 combines these possibilities with the ratios by which the weight of bare shell increases on stiffening and will help a practicing engineer to choose his optimum solution considering both economy and other practical limitations such as aesthetics and headroom. In many practical situations an engineer has to restrict the stiffener depth and also the number of stiffeners in either direction. Table 8 is prepared taking practical upper limits of $d_{st}/h = 4$ and $n_x = n_y = 6$ and will help a practicing engineer to decide on the number and depth of stiffeners which will economically achieve a given increase of the fundamental frequency of a bare shell.

Acknowledgement

The first author gratefully acknowledges the financial assistance of CSIR (India) through the Senior Research Fellowship vide Grant no. 9/96 (412) 2003-EMR-I.

References

- [1] N.S. Bardell, D.J. Mead, Free vibration of an orthogonally stiffened cylindrical shell—part II: discrete general stiffeners, *Journal of Sound and Vibration* 134 (1) (1989) 55–72.
- [2] Z. Mecitoğlu, M.C. Dökmeçi, Free vibrations of a thin stiffened, cylindrical shallow shell, *AIAA Journal* 30 (3) (1991) 848–850.
- [3] M.D. Olson, Efficient modelling of blast loaded stiffened plate and cylindrical shell structures, *Computers & Structures* 40 (5) (1991) 1139–1149.
- [4] G. Sinha, M. Mukhopadhyay, Finite element free vibration analysis of stiffened shells, *Journal of Sound and Vibration* 171 (4) (1994) 529–548.
- [5] J. Jiang, M.D. Olson, Vibration analysis of orthogonally stiffened cylindrical shells using super finite elements, *Journal of Sound and Vibration* 173 (1) (1994) 73–83.
- [6] D. Chakravorty, J.N. Bandyopadhyay, On the free vibration of shallow shells, *Journal of Sound and Vibration* 185 (4) (1995) 673–684.
- [7] D. Chakravorty, J.N. Bandyopadhyay, P.K. Sinha, Finite element free vibration analysis of point supported laminated composite cylindrical shells, *Journal of Sound and Vibration* 181 (1) (1995) 43–52.
- [8] D. Chakravorty, J.N. Bandyopadhyay, P.K. Sinha, Finite element free vibration analysis of doubly curved laminated composite shells, *Journal of Sound and Vibration* 191 (4) (1996) 491–504.
- [9] G. Sinha, M. Mukhopadhyay, Static and dynamic analysis of stiffened shells—a review, *Proceedings of the Indian National Science Academy* 61A (3 & 4) (1995) 195–219.

- [10] S. Goswami, M. Mukhopadhyay, Finite element free vibration analysis of laminated composite stiffened shell, *Journal of Composite Materials* 29 (18) (1995) 2388–2422.
- [11] M. Mukhopadhyay, S. Goswami, Transient finite element dynamic response of laminated composite stiffened shell, *The Aeronautical Journal of the Royal Aeronautical Society*, June/July 1996, pp. 223–233.
- [12] B.G. Prusty, S.K. Satsangi, Finite element transient dynamic analysis of laminated stiffened shells, *Journal of Sound and Vibration* 248 (2) (2001) 215–233.
- [13] R. Rikards, A. Chate, O. Ozolinsh, Analysis for buckling and vibrations of composite stiffened shells and plates, *Composite Structures* 51 (2001) 361–370.
- [14] M.S. Qatu, Recent research advances in the dynamic behaviour of shells: 1989–2000—part 1: laminated composite shells, *Applied Mechanics Reviews* 50 (4) (2002) 325–349.
- [15] M.S. Qatu, Recent research advances in the dynamic behaviour of shells: 1989–2000—part 2: Homogeneous shells, *Applied Mechanics Reviews* 50 (5) (2002) 415–434.
- [16] A.N. Nayak, J.N. Bandyopadhyay, Free vibration analysis and design aids of stiffened conoidal shells, *ASCE Journal of Engineering Mechanics* 128 (4) (2002) 419–427.
- [17] A.N. Nayak, J.N. Bandyopadhyay, On the free vibration of stiffened shallow shells, *Journal of Sound and Vibration* 255 (2) (2002) 357–382.
- [18] D. Chakravorty, J.N. Bandyopadhyay, P.K. Sinha, Applications of FEM on free and forced vibrations of laminated shells, *ASCE Journal of Engineering Mechanics* 124 (1) (1998) 1–8.
- [19] S. Sahoo, D. Chakravorty, Finite element bending behaviour of composite hyperbolic paraboloidal shells with various edge conditions, *Journal of Strain Analysis for Engineering Design* 39 (5) (2004) 499–513.
- [20] S. Sahoo, D. Chakravorty, Finite element vibration characteristics of composite hypar shallow shells with various edge supports, *Journal of Vibration and Control* 11 (2005) 1291–1309.
- [21] A.N. Nayak, J.N. Bandyopadhyay, Free vibration analysis of laminated stiffened shells, *ASCE Journal of Engineering Mechanics* 131 (1) (2005) 100–105.
- [22] A. Mukherjee, M. Mukhopadhyay, Finite element free vibration of eccentrically stiffened plates, *Computers and Structures* 30 (1988) 1303–1317.
- [23] M.S. Qatu, A.W. Leissa, Vibration studies for laminated composite twisted cantilever plates, *International Journal of Mechanical Sciences* 33 (11) (1991) 927–940.